Frontiers in Bioscience Landmark

Front. Biosci. (Landmark Ed) **2026**; 31(7): 50593
https://doi.org/10.31083/FBL50593

Original Research

Early Expansion of Monocytic Myeloid-Derived Suppressor Cells Predicts Survival in Sepsis and Is Possibly Associated With Activation of Endoplasmic Reticulum Stress Pathways

Juanli Liu[1,2], Tana Wuren[1], Xiaoyan Song[1], Xue Sun[3], Siqing Ma[2,*], Rili Ge[1,*]

[1]Research Center for High Altitude Medicine, Key Laboratory of High Altitude Medicine (Ministry of Education), Key Laboratory of Application and Foundation for High Altitude Medicine Research in Qinghai Province (Qinghai-Utah Joint Research Key Laboratory for High Altitude Medicine), Qinghai University, 81000 Xining, Qinghai, China
[2]Department of Critical Care Medicine, Qinghai Provincial People's Hospital, 810000 Xining, Qinghai, China
[3]Department of Nephrology, Affiliated Hospital of Qinghai University, 810000 Xining, Qinghai, China
*Correspondence: siqing177@sina.com (Siqing Ma); geriligao@hotmail.com (Rili Ge)
Academic Editor: Vijay Kumar
Submitted: 1 February 2026 Revised: 19 May 2026 Accepted: 29 May 2026 Published: 21 July 2026

Abstract

Background: Sepsis is characterized by profound immune dysregulation, in which myeloid-derived suppressor cells (MDSCs) serve as key regulators of the host immune response. However, the prognostic significance of distinct MDSC subsets during the early phase of sepsis remains incompletely understood. **Methods:** In this prospective cohort study, flow cytometry was used to quantify circulating MDSC subsets in sepsis patients within 24 hours of intensive care unit (ICU) admission and in healthy control subjects. Patients were followed to establish 90-day survival, and the prognostic significance of MDSC subset frequencies on admission was evaluated using receiver operating characteristic (ROC) curve analysis and Cox regression models. Multivariate Cox models were adjusted for disease severity scores. A murine cecal ligation and puncture (CLP) model of sepsis was also used to investigate temporal and tissue-specific MDSC dynamics and to examine endoplasmic reticulum (ER) stress-related signaling within these cells. **Results:** Compared with healthy controls, patients with sepsis exhibited the marked expansion of circulating MDSCs, including both polymorphonuclear and monocytic subsets. Among these, the proportion of circulating monocytic MDSCs (M-MDSCs) on ICU admission was significantly higher in 90-day survivors than in non-survivors. After adjusting for disease severity and other clinical variables, higher M-MDSC frequencies were independently associated with lower 90-day mortality. ROC curves confirmed the ability of the M-MDSC proportion to predict 90-day mortality. In the CLP model, MDSC subsets displayed temporal and tissue-specific dynamics that differed between the acute and recovery phases of sepsis. MDSCs isolated from septic mice exhibited ER stress-related pathway activation in the spleen and bone marrow. Collectively, these findings suggest that early M-MDSC expansion represents a distinct immunological phenotype associated with favorable outcomes in sepsis. **Conclusions:** An early increase in circulating M-MDSCs is associated with improved 90-day survival in patients with sepsis. These findings underscore the dynamic, context-dependent role of M-MDSCs in sepsis, indicating that early immunoregulatory responses, possibly associated with activation of ER stress pathways, may represent an adaptive mechanism leading to favorable clinical outcomes.

Keywords: sepsis; myeloid-derived suppressor cells; monocytic myeloid-derived suppressor cells; prognosis; endoplasmic reticulum stress

1. Introduction

Sepsis remains a leading cause of morbidity and mortality worldwide and a major challenge in critical care medicine [1]. Despite marked improvements in antimicrobial treatment, organ support, and early detection methods, sepsis patients continue to experience poor short and long-term outcomes, with mortality rates remaining unacceptably high [2]. Sepsis is associated with diverse clinical manifestations and host responses to infection that remain major challenges to improving sepsis patient outcomes, highlighting the need for a comprehensive understanding of sepsis-related immune dysregulation and dependable biomarkers that offer insight into host immune status rather than simply reflecting disease severity [1,3,4].

Sepsis involves a complex, dynamic interaction between heightened inflammatory activity and the suppression of immune activity [5,6]. While early hyperinflammatory responses may contribute to acute organ injury, accumulating evidence indicates that many patients rapidly develop features of immune dysfunction, including impaired antigen presentation, lymphocyte exhaustion, and altered myeloid cell function [7,8,9,10]. Importantly, these immune alterations are not uniform across patients or over time, suggesting that distinct immune phenotypes may underlie divergent clinical trajectories and outcomes [11,12].

Myeloid-derived suppressor cells (MDSCs) play a crucial role in regulating immune responses across diverse pathological conditions such as cancer, chronic infections,

and inflammatory diseases [13,14]. MDSCs are immature myeloid cells that can be broadly categorized into polymorphonuclear (P-MDSCs) and monocytic (M-MDSCs) subsets, with each possessing unique phenotypic and functional traits [15]. Through mechanisms such as the suppression of T-cell activation, the modulation of cytokine production, and the regulation of innate immune responses, MDSCs can profoundly shape host immunity [16,17]. In sepsis, circulating MDSCs frequently expanded; undergo expansion, although their clinical significance continues to be the subject of scholarly debate [8,18].

Previous studies investigating MDSCs in sepsis have yielded inconsistent and sometimes conflicting results [19,20,21,22,23]. Several reports have associated increased MDSC levels with immune paralysis, secondary infections, and adverse outcomes [24,25,26], whereas others have suggested neutral or even protective roles for specific MDSC subsets [27,28,29]. These discrepancies may reflect differences in study design, patient populations, timing of immune assessment, and analytical strategies [15,30]. In particular, many studies have focused on total MDSCs or on measurements obtained during the later phases of sepsis, potentially obscuring the distinct and time-dependent roles of individual MDSC subsets during the early course of the disease.

Among MDSC subsets, M-MDSCs have been the focus of particularly intensive study due to their potent immunomodulatory capacity and their close relationship with circulating monocytes. Experimental and clinical data suggest that M-MDSCs may exert context-dependent effects, mediating the balance between inflammatory injury and immune regulation in a manner that depends both on disease stage and microenvironmental cues [31]. However, it remains unclear as to whether early alterations in circulating M-MDSCs are of prognostic significance in sepsis or how these cells shape and/or respond to the underlying biological processes that define this devastating condition.

Cellular stress responses are increasingly linked to the pathophysiology of sepsis. The unfolded protein response and endoplasmic reticulum (ER) stress are essential for the preservation of cellular homeostasis during inflammation, hypoxia, and metabolic disturbances [32,33]. Recent reports suggest that ER stress signaling can influence immune cell differentiation and function, including that of myeloid cells [34]. The potential role of ER stress pathways in the modulation of sepsis-associated MDSC responses, however, has not been well characterized.

This prospective cohort analysis was developed to examine the early expansion of circulating MDSC subsets in sepsis patients and to clarify how these myeloid cell dynamics relate to 90-day mortality. In addition, a cecal ligation and puncture (CLP)-induced murine sepsis model was employed to examine temporal and tissue-specific MDSC dynamics and MDSC-intrinsic ER stress-related signaling, complementing our clinical observations. The overall goal of this study was to determine the prognostic significance and biological traits associated with early M-MDSC expansion in sepsis through the systematic evaluation and integration of clinical and experimental evidence.

2. Materials and Methods

2.1 Study Design and Population

This prospective cohort study was conducted in the intensive care unit (ICU) of Qinghai Provincial People's Hospital, Xining, China, from February to December 2024. Patients were consecutively screened and enrolled at ICU admission according to predefined inclusion and exclusion criteria. Sepsis was diagnosed in accordance with the Sepsis-3 definition. Eligible participants were adults aged 18–80 years. Patients were excluded if they were pregnant or lactating, had a history of malignancy or autoimmune disease, had hematological disorders, HIV infection, or were receiving immunosuppressive therapy.

Of the 100 patients screened for eligibility, 25 were excluded during screening, including 5 who died within 24 hours of ICU admission, 10 with malignancies, 3 with intracranial infections, 3 with skin and soft tissue infections, and 4 with HIV infection. In addition, 5 patients were lost to follow-up. Ultimately, 70 patients with sepsis were included in the final analysis. A total of 21 age-matched healthy individuals without evidence of acute infection were also included. Patients were followed for up to 90 days after ICU admission. Clinical data were systematically collected, including demographic characteristics, baseline clinical parameters, laboratory findings, and 90-day all-cause mortality.

2.2 Sample Storage

Blood samples from patients were obtained within 24 hours of ICU admission. Venous blood (2 mL) was drawn into EDTA-containing tubes. The samples were centrifuged, and the serum was stored at –80 °C for future experiments.

2.3 Flow Cytometry

Flow cytometry was conducted as reported previously [15], with application-specific antibodies. We utilized the BV510-Zombie Aqua Fixable Viability Kit (BioLegend, 423102) and performed MDSC phenotyping via five-color flow cytometry with the following antibodies: FITC-anti-CD11b (BD, 557396), BV421-anti-CD33 (BioLegend, 366621), PerCP-Cy5.5-anti-HLA-DR (BioLegend, 307630), PE-anti-CD14 (BioLegend, 367104), and PE-Cy7-anti-CD15 (BioLegend, 301924). The proportions of MDSCs and associated subtypes were detected using a BD Aria III flow cytometer, and the resulting data were analyzed in FlowJo v10.8.1 (BD Biosciences, Franklin Lakes, NJ, USA).

2.4 Phenotypic Analysis

Whole blood was stained as previously described [15]. Total MDSCs were identified as $CD33^{+}CD11b^{+}HLA\text{-}DR^{-/low}$ cells. M-MDSCs were defined as being $CD14^{+}$, while P-MDSCs were identified as $CD14^{-}CD15^{+}$ cells. Flow cytometric analyses were performed using a standardized gating strategy, although inter-assay variability cannot be completely excluded.

2.5 Inflammation Index Measurement

Human serum concentrations of IL-6, IL-1β, IL-10, and IL-8 were quantified using the CBA Human Inflammatory Cytokines Kit (cat/# 551811/1267105, BD, New Jersey, USA). Briefly, after vortexing for 10 seconds, 10 µL of microspheres were extracted from each tube. Serum samples were processed by centrifugation, treated with a plasma enhancement solution, diluted, and incubated with microspheres and PE-conjugated inflammatory factor antibodies, with intermittent washes, to prepare them for downstream analysis. TNF-α levels were assessed using an appropriate kit (JLW10208; Jonln, Shanghai, China). Plasma levels of other cytokines were assessed using commercial ELISA kits as per the manufacturer's guidelines. All samples were analyzed in duplicate.

2.6 Murine Cecal Ligation and Puncture (CLP) Model

The study was carried out in accordance with the ARRIVE guidelines. Male C57BL/6J mice (10–14 weeks, 22–28 g) were obtained from Jiangsu Huachuang Xinuo Pharmaceutical Co., Ltd. In Suzhou, China. Prior to experimental use, mice were acclimated for at least three days in the Plateau Medicine Research Center's animal facility, which maintained a controlled temperature (18–24 °C) and humidity (50–60%) with a 12-hour light/dark cycle. Animals were randomly assigned to three subgroups based on time post-surgery: Sham, CLP 12 h, and CLP 168 h (n = 18/group). The experimental unit was each individual mouse. Sample size was based on previous similar CLP studies and pilot experimental data in our laboratory. All surgical procedures were performed under general anesthesia with isoflurane (veterinary drug approval No. 020037015, RWD) using an RWD Life Science animal gas anesthesia system (Model number R583S, Shanghai, China). CLP was performed following a previously described protocol [35]. The key steps of the procedure were as follows: A 1-cm midline abdominal incision was made to expose the cecum, which was ligated approximately 1 cm from the distal end and punctured with a 22-gauge needle approximately 0.2 cm distal to the ligation. Following surgery, all mice underwent subcutaneous resuscitation with 1 mL of sterile 0.9% saline (Sichuan, China). Animals were provided unrestricted access to food and water throughout the study.

To establish the sepsis model, we employed the CLP model, a polymicrobial sepsis model that more closely mimics the clinical pathophysiology of human sepsis. In addition, throughout the experimental process, organ injury markers, inflammatory cytokine levels, and changes in MDSCs and their subsets were evaluated at multiple time points after CLP. The 12-hour time point was considered to represent the acute hyperinflammatory phase, characterized by severe organ dysfunction, cytokine storm, and peak innate immune activation, and was therefore selected to represent the early acute inflammatory stage of sepsis. In contrast, at 7 days after CLP, surviving animals had entered a stage of immune remodeling, during which MDSC expansion became more prominent. Accordingly, this time point was considered more suitable for investigating PD-1/PD-L1 signaling and sepsis-associated immunosuppression. Therefore, the primary focus of the present study was to compare the acute inflammatory phase and the partial recovery-associated immune remodeling phase during sepsis progression, and the 12 h and 7-day time points were selected accordingly.

2.7 Experiment Animal Sampling

Mice were anesthetized with isoflurane (inhaled concentration 1.5%) (20240606, China) using an inhalational animal anesthesia system (R583S, China). Whole blood was collected via pericardiocentesis under deep anesthesia, followed by transfer into EDTA-coated tubes for anticoagulation. Euthanasia was subsequently confirmed by exsanguination, in accordance with institutional guidelines for animal care and use. Spleens were collected and mechanically dissociated [36] with a 5 mL syringe plunger to create single-cell suspensions. Bone marrow (BM) cells were extracted by washing the femur and tibia shafts with phosphate-buffered saline (PBS, China), followed by brief centrifugation. Red blood cells from all tissues were lysed. The resulting cell suspensions were subsequently processed for flow cytometric analysis.

2.8 Measurement of Organ Injury Markers

Serum was extracted by centrifuging blood samples at 2000 ×g for 20 minutes. An automated biochemical analyzer was employed as directed to assess serum levels of organ injury markers, including creatine kinase (CK), creatine kinase isoenzyme (CK-MB), lactate dehydrogenase (LDH), aspartate aminotransferase (AST), alanine aminotransferase (ALT), blood urea nitrogen (BUN), and creatinine (Cr).

2.9 Serum Inflammatory Cytokine Analyses

Serum levels of IL-6, IL-10, and TNF were assessed using the BD™ CBA Mouse Inflammatory Kit (552364, BD, USA) following the manufacturer's guidelines.

2.10 Murine MDSC Subset Staining

BM and spleen cell suspensions were prepared according to established methods. Briefly, ~1×10^{6} cells in 100 µL of staining buffer were stained with the Zombie Aqua™

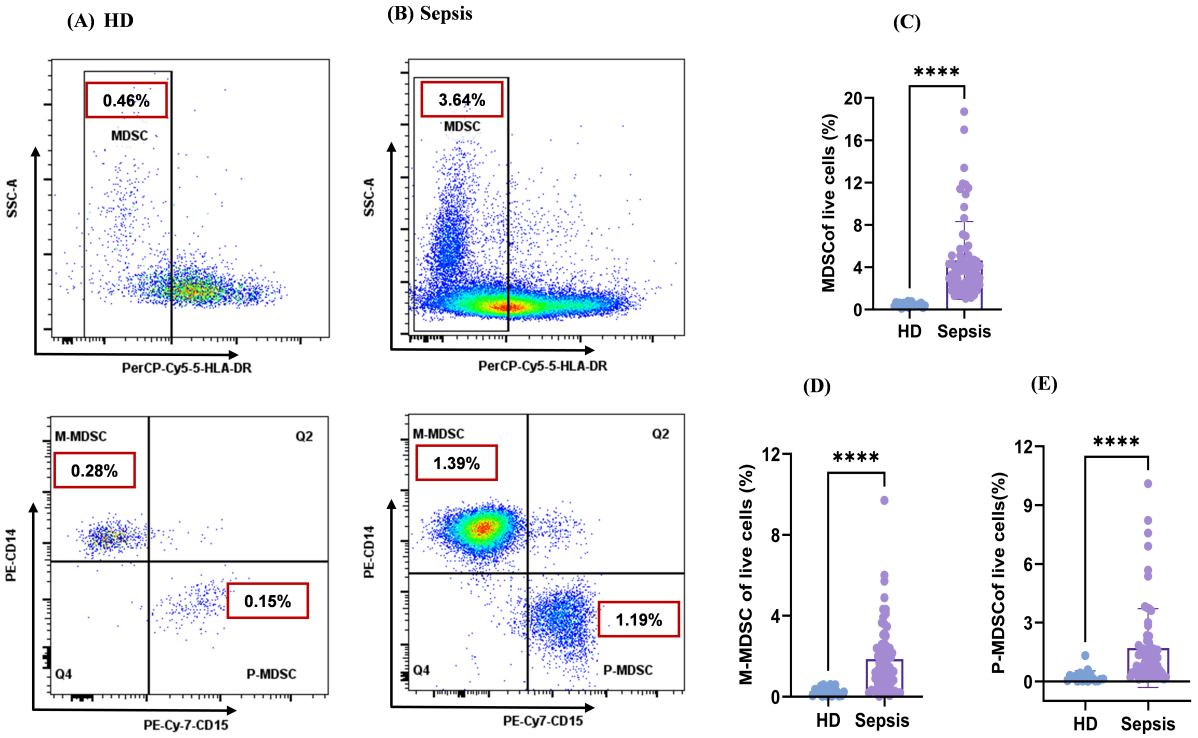

Fig. 1. Circulating MDSC subset frequencies in sepsis patients and healthy donors. (A) shows the percentage of total MDSCs, M-MDSCs and P-MDSCs in the healthy donors (n = 21), while (B) presents these percentages in sepsis patients (n = 70). (C) Compares MDSC percentages between healthy donors and sepsis patients. (D) Compares M-MDSC percentages between healthy donors and sepsis patients. (E) Compares P-MDSC percentages between healthy donors and sepsis patients. Data are presented as the median with interquartile range (IQR) and were compared with the Mann-Whitney U test. ****$p < 0.0001$.

(cat/# 423102/B395874, BioLegend, USA) to exclude dead cells. Fc receptor blocking was performed for 10 minutes using Mouse TruStain FcX™ (cat/# 101320/B411434, BioLegend, USA). Cells were then incubated with appropriate antibodies in a 100 µL volume at 4 °C for 30 minutes in the dark, washed twice (500 ×g, 5 minutes), and resuspended in 500 µL of PBS for acquisition. Antibodies used for this study included FITC anti-mouse/human CD11b (cat/# 101205/B324795), PerCP-Cy5.5 anti-mouse CD45 (cat/# 103132/B370639), PE anti-mouse Ly6C (cat/# 128008/B313796), and PE/Cy7 anti-mouse Ly6G (cat/# 127618/B351626), all from BioLegend, USA.

Mouse MDSC populations were defined as in a prior study [15]:

M-MDSCs are identified based on the markers $CD45^+$, $CD11b^+$, $Ly6G^-$, and $Ly6C^+$

P-MDSCs are distinguished by the markers $CD45^+$, $CD11b^+$, $Ly6G^+$, and $Ly6C^-$

2.11 Isolation of $CD11b^+Gr\text{-}1^+$ Cells

$CD11b^+Gr\text{-}1^+$ cells were isolated from mouse spleens and bone marrow using the Easy Sep™ Mouse MDSC Isolation Kit (cat/# 19867/1000171555, Canada) following the manufacturer's instructions. Post-sort purity was verified by flow cytometry.

2.12 Western Blotting

$CD11b^+Gr\text{-}1^+$ cells were lysed in 1× RIPA lysis buffer containing 1 mM PMSF, and 1× Phosphatase Inhibitor Cocktail 2. Lysates were then centrifuged, and protein concentrations were determined using an Enhanced BCA Protein Assay Kit, after which samples (25–30 µg per lane) were separated via electrophoresis and transferred to PVDF membranes. After blocking with 5% BSA for 1 hour, membranes were incubated overnight with the following antibodies: Anti-GRP78/Bip (cat/# C50812/10, 1:1000, CST, USA), Anti-XBP1 (cat/# ab220783/1053976-17, 1:1000, Abcam, USA), Anti-phospho-eIF2α (cat/# s51/6, 1:1000, CST, USA), Anti-eIF2α (cat/# C3294/7, 1:1000, CST, USA), Anti-ATF4 (cat/# C11815/5, 1:1000, CST, USA), Anti-ATF6 (cat/#66563-1-Ig/10042149, 1:1000, Proteintech, USA), or Anti-β-actin (cat/# 20536-1-AP/9300014001, 1:5000, Proteintech, China). After washing, membranes were incubated with appropriate secondary antibodies for 1 hour, and signal intensity levels were quantified using ImageJ 1.54m (National Institutes of Health, Bethesda, MD, USA).

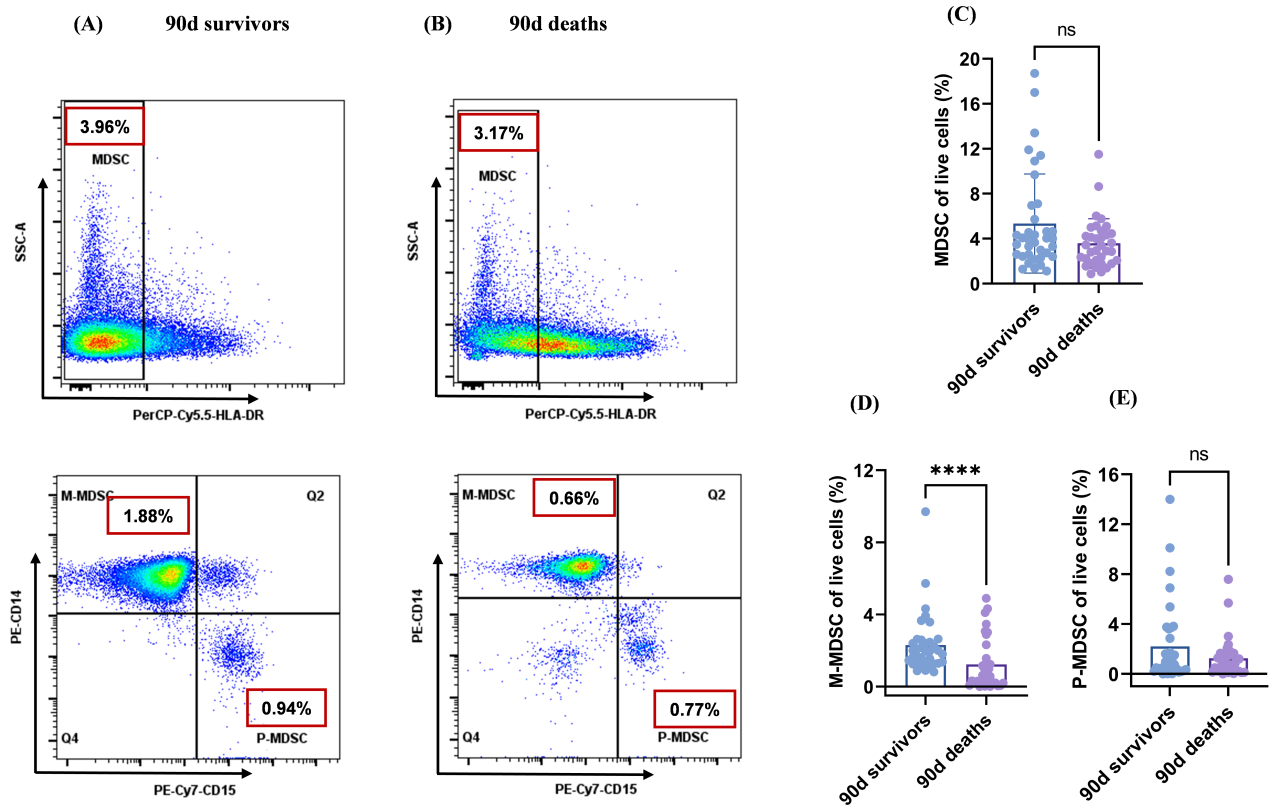

Fig. 2. Comparison of MDSC subsets and clinical outcomes between 90-day survivors and non-survivors. (A) Shows the percentage of MDSCs, M-MDSCs and P-MDSCs in the 90-day survivors, while (B) presents these percentages in the 90-day non-survivors. (C) Compares MDSC percentages between the 90-day survivors and the 90-day non-survivors. (D) Compares M-MDSC percentages between the 90-day survivors and the 90-day non-survivors. (E) Compares P-MDSC percentages between the 90-day survivors and the 90-day non-survivors. Data are presented as the median with the interquartile range (IQR). The Mann-Whitney U test was utilized for group comparisons. ns, $p > 0.05$; ****$p < 0.0001$.

2.13 Statistical Analysis

GraphPad Prism 9.4 (GraphPad Software, San Diego, CA, USA) and SPSS 28.0 (IBM, Corp. Armonk, NY, USA) were utilized for statistical analyses. The clinical data were analyzed using median (IQR) and the Mann–Whitney U test, and the animal experimental data are expressed as mean ± standard deviation (SD). One-way ANOVAs were used when comparing multiple groups with normally distributed data. Factors associated with 90-day survival were identified via regression. Predictive performance was evaluated using Receiver Operating Characteristic (ROC) curves and the Youden index, while survival differences were analyzed with Kaplan-Meier curves. All statistical tests were two-sided, and a p-value < 0.05 was considered statistically significant.

3. Results

3.1 Basic Patient Characteristics

A total of 70 sepsis patients were enrolled in the study. All patients were admitted to the ICU within 24 hours of sepsis diagnosis, with 21 healthy donors (HD) serving as controls. Among the sepsis cohort, 36 patients survived, and 34 patients died within 90 days after ICU admission. Baseline characteristics of the population are presented in **Supplementary Table 1**.

Non-survivors exhibited a higher prevalence of hypertension compared to survivors. At the time of ICU admission, non-survivors had significantly elevated Acute Physiology and Chronic Health Evaluation (APACHE) II and Sequential Organ Failure Assessment (SOFA) scores. In addition, lactate concentrations and plasma levels of inflammatory cytokines were significantly higher in non-survivors relative to survivors, with the exception of IL-1β (Table 1).

3.2 Expansion of Circulating MDSC Subsets in Patients With Sepsis

Blood samples were collected from sepsis patients within 24 hours of ICU admission, and flow cytometric staining was performed within 30 minutes of sample collection. Gating strategy MDSC subset (**Supplementary Fig. 1**). Compared with healthy donors, patients with sepsis exhibited robust expansion of total MDSCs (3.64% vs 0.46%), P-MDSCs (1.19% vs 0.15%), and M-MDSCs (1.39% vs 0.28%) (all $p < 0.0001$) (Fig. 1A–E).

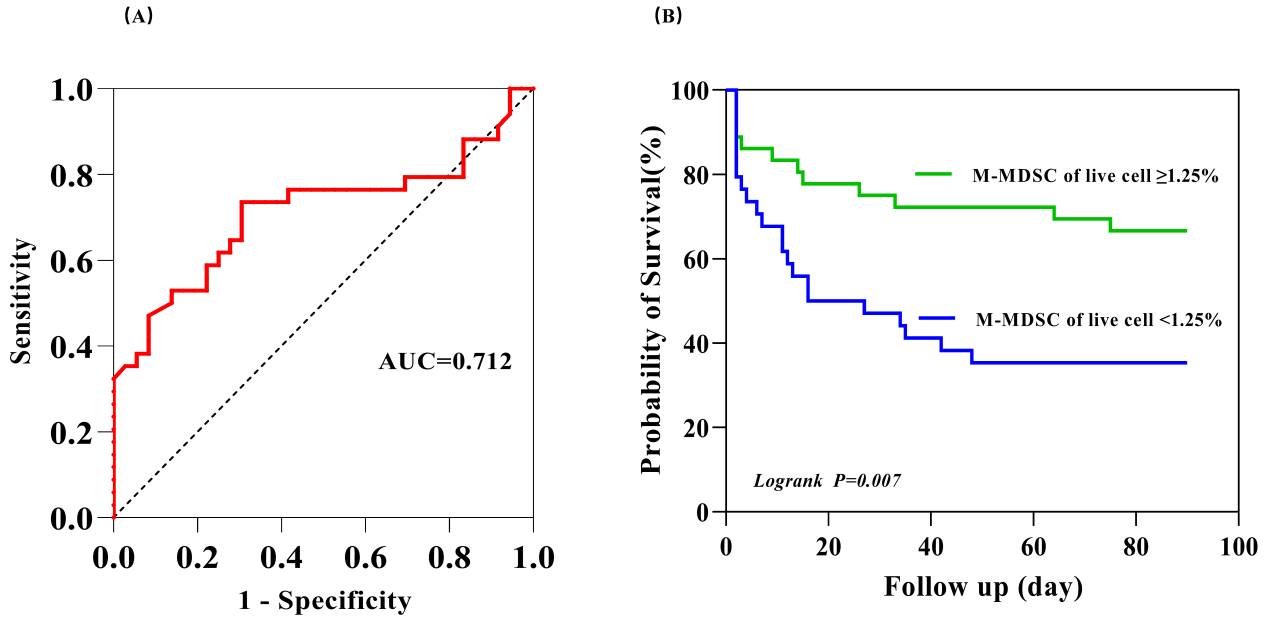

Fig. 3. Prognostic value of M-MDSC proportion as a predictor of 90-day mortality in sepsis. (A) Receiver operating characteristic (ROC) curve evaluating the predictive performance of M-MDSC proportion for 90-day mortality. (B) Kaplan-Meier survival curves for patients stratified using the optimal M-MDSC cut-off value (1.25%).

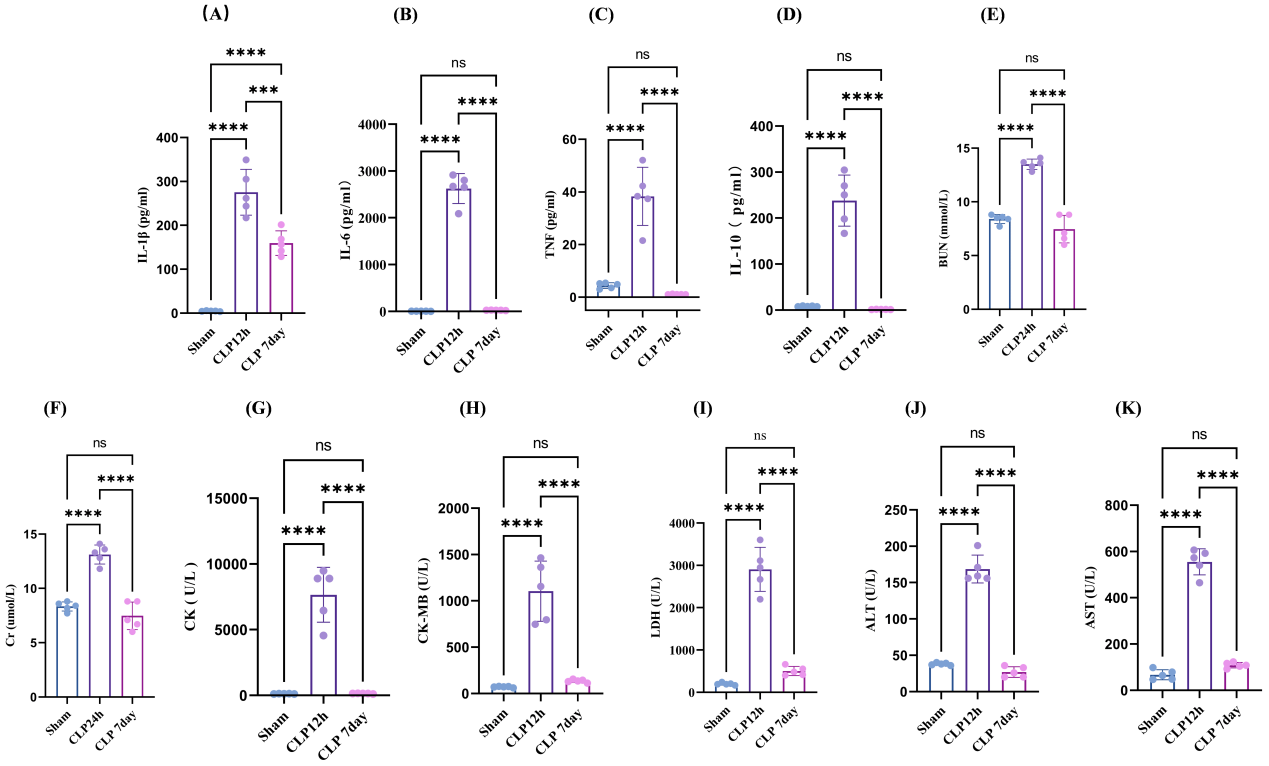

Fig. 4. Serum inflammatory cytokine levels and organ function indicators in CLP model mice at 12 h and 7 days post-CLP. Serum levels of seven organ-specific injury markers were measured across the Sham, CLP 12 h, and CLP 7 day groups (n = 5 per group). (A) IL-1β; (B) IL-6; (C) TNF; (D) IL-10; (E) BUN; (F) Cr; (G) CK; (H) CK-MB; (I) LDH; (J) ALT; (K) AST. Data are expressed as mean ± standard deviation. One-way ANOVA was used for comparing multiple groups' data. ns, not significant, ***$p < 0.001$, ****$p < 0.0001$. CLP, cecal ligation and puncture.

Table 1. Baseline demographic and clinical characteristics of patients with sepsis and healthy controls.

Contents	Healthy donors [M (P_{25}, P_{75})]	Sepsis patients [M (P_{25}, P_{75})]		*p*-value
		90-d survivors	90-d non-survivors	
Number of patients	21	36	34	-
Gender (male/female)	11/10	24/12	22/12	
Age (years)	57 (50–60)	58 (45–69)	59 (52–71)	0.581
Hypertension, n (%)	6 (29%)	6 (17%)	13 (38%)	0.043
Diabetes, n (%)	5 (23%)	9 (25%)	8 (24%)	0.259
Hypertension and Diabetes n (%)	3 (14%)	4 (11%)	4 (12%)	0.457
APACHE II score	-	12 (9, 14)	15 (12, 20)	0.006
SOFA score	-	6.5 (4, 8)	9.5 (6, 12)	0.000
Neutrophils ($\times 10^9$/L)	2.94 (2.42, 3.87)	9.49 (6.50, 14.95)	8.10 (5.27, 13.07)	0.204
Monocytes ($\times 10^9$/L)	0.40 (0.34, 0.58)	0.36 (0.26, 0.59)	0.51 (0.30, 0.69)	0.192
Lactate (mmol/L)	-	1.20 (0.90,1.88)	2.15 (1.70, 3.53)	0.000
TNF-α (pg/mL)	25.83 (22.62, 32.42)	1379.25 (644.63, 4297.46)	5884.25 (1885.90, 7911.15)	0.000
IL-6 (pg/mL)	2.38 (1.17, 3.63)	101.9 (43.1, 362.7)	734.3 (188.7, 2420.3)	0.003
IL-1β (pg/mL)	0.39 (0.26,1.02)	6.30 (4.90, 8.40)	7.40 (2.20, 11.90)	0.948
IL-8 (pg/mL)	3.99 (2.99, 6.446)	27 (20, 39)	210 (119, 500)	0.000
IL-10 (pg/mL)	0.48 (0.32, 1.30)	7.50 (3.70, 13.10)	56.60 (29.60, 145.10)	0.000
IL-7 (pg/mL)	29.34 (17.01, 54.84)	262 (140, 613)	188 (72, 278)	0.007
IL-15 (pg/mL)	15.60 (10.60, 17.90)	108 (48, 195)	180 (53, 534)	0.026

Comparison of demographic characteristics, laboratory markers, severity scores, lactate concentration, and plasma cytokines (TNF-α, IL-6, IL-1β, IL-8, IL-10, IL-7, IL-15) between survivors and non-survivors at 90 days. Data are expressed as median (IQR) P25 and P75 represent the 25th and 75th percentiles (%). Statistical significance was determined using the Mann-Whitney U test. *p*-values indicate comparisons between 90-day survivors and non-survivors. TNF-α, Tumor Necrosis Factor-α; IL, Interleukin.

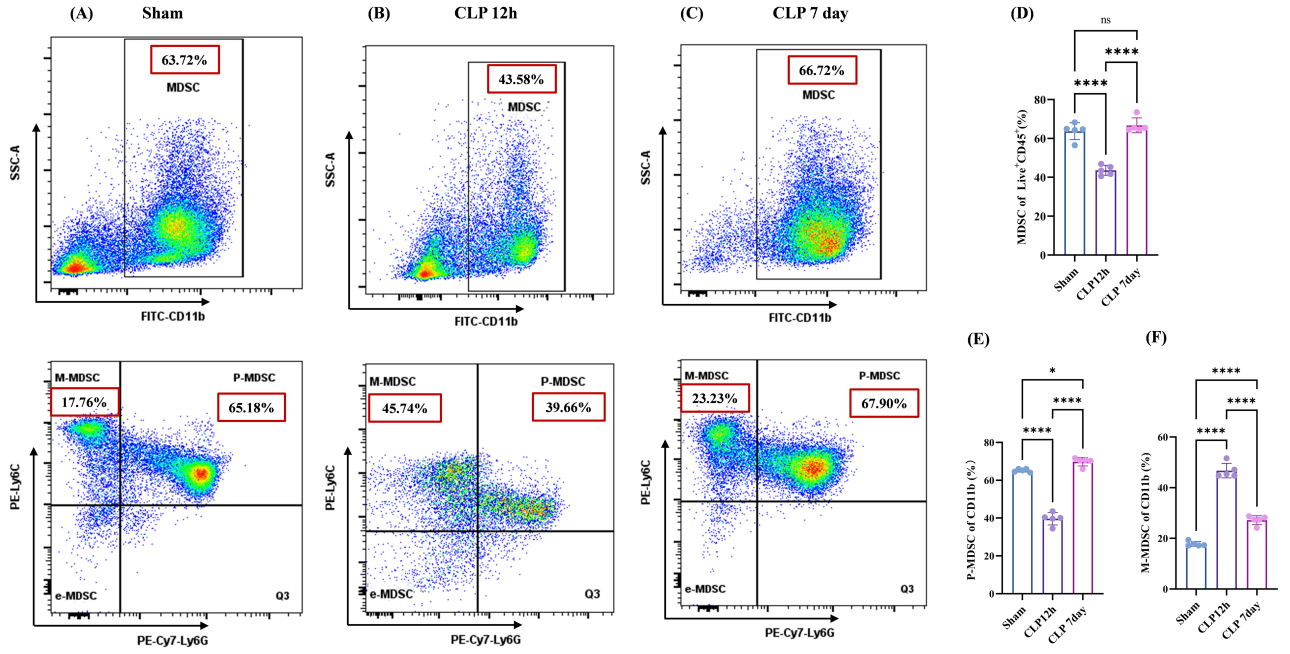

Fig. 5. The expression of MDSCs and their subsets in mouse bone marrow post-CLP. (A) Shows the percentage of MDSCs, M-MDSCs and P-MDSCs in the Sham group, while (B) presents these percentages in the CLP 12-hour group. (C) Depicts the percentages in the CLP 7-day group. (D) Compares MDSC proportions across the Sham, CLP 12-hour, and 7-day groups, and (E,F) provide a comparison of P-MDSC and M-MDSC proportions among these groups (n = 5 per group). Data are expressed as mean ± standard deviation. One-way ANOVA was used for comparing multiple groups' data. Significance levels are indicated as follows: ns, $p > 0.05$; *$p < 0.05$; ****$p < 0.0001$.

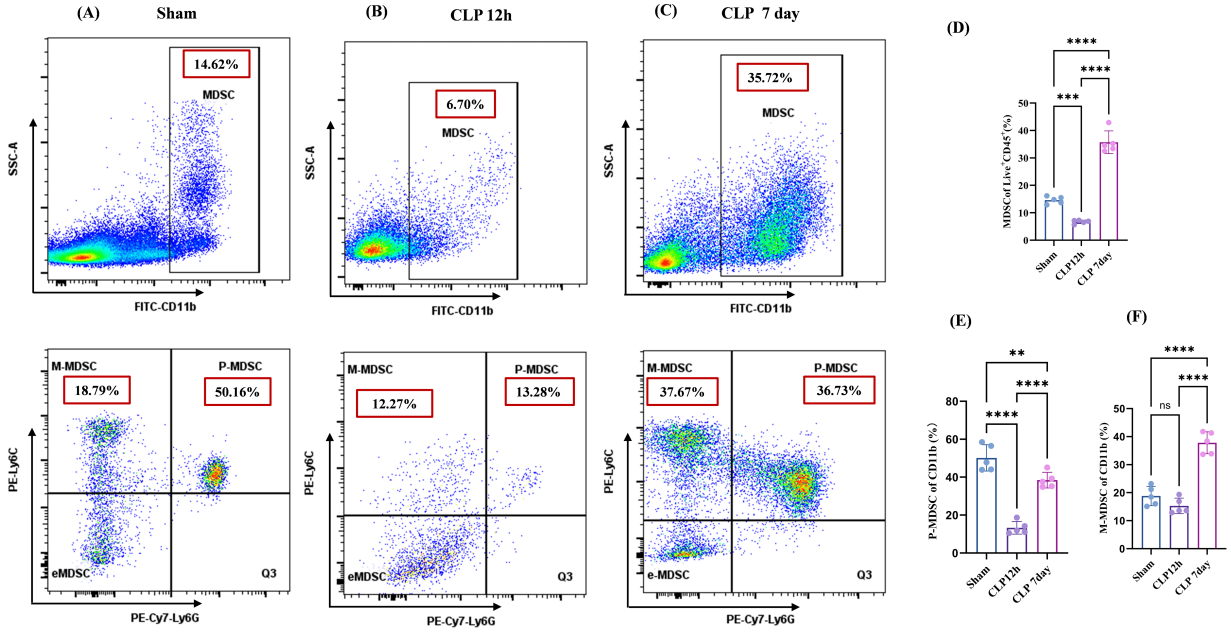

Fig. 6. The expression of MDSCs and their subsets in the spleen of mice post-CLP. (A) Shows the percentage of MDSCs, M-MDSCs and P-MDSCs in the Sham group, while (B) presents these percentages in the CLP 12-hour group. (C) Depicts the percentages in the CLP 7 -day group. (D) Compares MDSC proportions across the Sham, CLP 12-hour, and 7-day group, (E,F) provide a comparison of P-MDSC, M-MDSC proportions among these groups (n = 5 per group). Data are expressed as mean ± standard deviation. One-way ANOVA was used for comparing multiple groups' data. Significance levels are indicated as follows: ns, $p \geq 0.05$; **$p < 0.01$; ***$p < 0.001$, ****$p < 0.0001$.

3.3 Association Between M-MDSC Levels and 90-Day Survival

To explore the association between MDSC subsets and clinical outcomes, sepsis patients were stratified according to 90-day survival status. As shown in Fig. 2, the proportion of circulating M-MDSCs at ICU admission was significantly higher in 90-day survivors than in non-survivors ($p < 0.0001$). Conversely, the total MDSCs and P-MDSCs did not differ significantly between survivors and non-survivors (Fig. 2B,C,E). Among circulating MDSC subsets, only M-MDSC levels were significantly elevated, with an approximately three-fold increase in survivors relative to non-survivors (Fig. 2A,B,D).

3.4 Prognostic Performance of M-MDSCs in Evaluating 90-Day Mortality

We divided the patients with sepsis based on their survival status within 90 days (0 for survival; 1 for death). Age, hypertension, diabetes, APACHE II score, SOFA score, Albumin, Monocytes, PCT (Procalcitonin), MDSC, M-MDSC, and P-MDSC were used as independent variables for univariate Logistic regression analysis. The results showed that SOFA score, APACHE II score, M-MDSC, Albumin, PT, PCT, and CRP (C-reactive protein) were all factors influencing the 90-day survival of sepsis patients ($p < 0.05$). For multivariate Logistic regression analysis of these indicators (SOFA score, APACHE II score, M-MDSC, Albumin, PT, PCT, CRP), the results showed that M-MDSC remained an independent influencing factor for 90-day survival of sepsis (**Supplementary Table 2**).

The prognostic value of circulating M-MDSCs was further assessed by receiver operating characteristic (ROC) curve analysis. At ICU admission, the proportion of M-MDSCs showed moderate discriminative ability for predicting 90-day mortality, with an AUC of 0.712 (95% CI: 0.584–0.839, $p = 0.002$) (Fig. 3A). The Youden index identified 1.25% of peripheral blood live cells as the optimal cut-off value for the M-MDSC proportion.

Based on this cutoff, patients were stratified into low (<1.25%) and high (≥1.25%) M-MDSC groups. Kaplan-Meier survival analysis showed significantly lower 90-day survival in patients with low M-MDSC levels than in those with high M-MDSC levels (Fig. 3B).

3.5 Independent Association Between M-MDSC Frequency and All-Cause Mortality

The results of univariate Cox proportional hazards analyses conducted to identify variables linked to 90-day mortality are presented in Table 2. Disease severity scores, selected laboratory parameters, inflammatory cytokine levels, and the proportion of circulating M-MDSCs were all significantly associated with mortality in these univariate analyses.

Table 2. COX regression analysis of sepsis patients with different prognoses.

Variable	Univariate analysis		Multivariate analysis	
	HR (95% CI)	*p*-value	HR (95% CI)	*p*-value
P-MDSC of live cell	0.885 (0.736–1.063)	0.191		
M-MDSC of live cell	0.743 (0.554–0.997)	0.048	0.696 (0.520–0.932)	0.015
SOFA score	1.173 (1.081–1.276)	0.000	1.126 (1.027–1.234)	0.011
APACHE II score	1.093 (1.037–1.152)	0.001	1.096 (1.030–1.1672)	0.004
CRP (mg/dL)	1.000 (0.997–1.003)	0.861		
PCT (ng/mL)	1.011 (1.002–1.021)	0.020	1.011 (1.000–1.022)	0.060
Lac (mmol/L)	1.741 (1.372–2.210)	0.000	1.470 (1.056–2.047)	0.023
Albumin (g/L)	0.919 (0.860–0.986)	0.014	0.977 (0.900–1.060)	0.746
IL-8 (pg/mL)	1.001 (1.000–1.001)	0.000	1.001 (1.000–1.001)	0.000

Univariate and multivariate Cox proportional hazards analysis evaluating demographic characteristics, laboratory values, cytokine levels, severity scores, and MDSC subset proportions for associations with 90-day mortality. Hazard ratios (HRs), 95% confidence intervals (CIs), and *p*-values are reported. Due to the large numerical range of cytokine concentrations, hazard ratios per unit increase appear close to 1. PCT, procalcitonin; CRP, C-reactive protein.

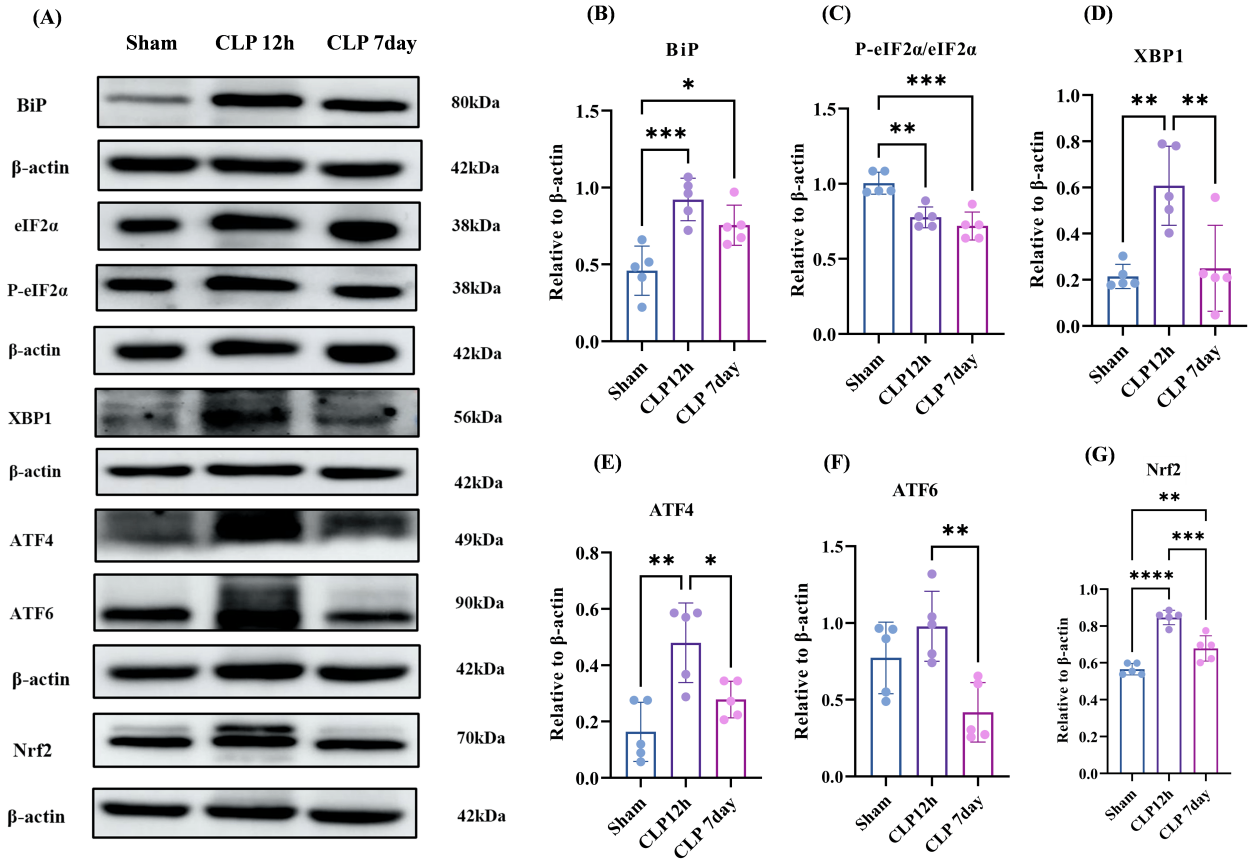

Fig. 7. Upregulation of ER stress-related proteins in splenic CD11b$^+$Gr-1$^+$cells. Six ER stress-related proteins were analyzed by Western blotting in splenic CD11b$^+$Gr-1$^+$ cells from the Sham, CLP 12 h and CLP 7-day groups (n = 5 per group). (A) Six endoplasmic reticulum stress proteins; (B) BIP expression among the three groups; (C) P-eIF2α/eIF2α expression among the three groups; (D) XBP1 expression among the three groups; (E)ATF4 expression among the three groups; (F) ATF6 expression among the three groups; (G) Nrf2 expression among the three groups. Data are presented as mean ± standard deviation. One-way ANOVA was used for comparing multiple groups' data. *$p < 0.05$, **$p < 0.01$, ***$p < 0.001$, ****$p < 0.0001$.

Variables with a $p < 0.05$ in univariate analyses were included in the multivariate Cox regression model. After adjustment for disease severity scores and relevant clinical variables, the proportion of circulating M-MDSCs re-

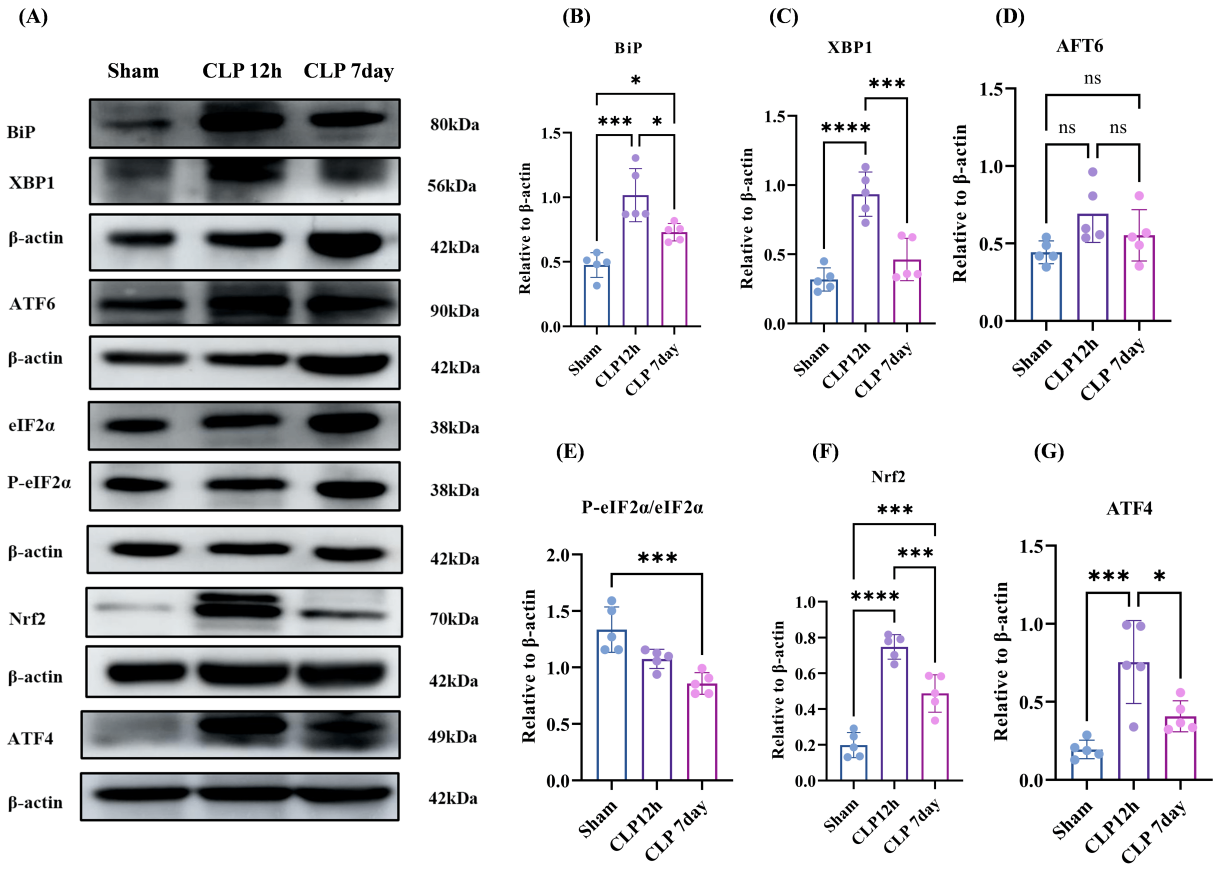

Fig. 8. Upregulation of ER stress-related proteins in bone marrow CD11b$^+$Gr-1$^+$cells. Six ER stress-related proteins were analyzed by Western blotting in bone marrow CD11b$^+$Gr-1$^+$ cells from the Sham, CLP 12-h, and CLP 7-day groups (n = 5 per group). (A) Six endoplasmic reticulum stress proteins; (B) BIP expression among the three groups; (C) XBP1 expression among the three groups; (D) ATF6 expression among the three groups; (E) P-eIF2α/eIF2α expression among the three groups; (F) Nrf2 expression among the three groups; (G) ATF4 expression among the three groups. Data are presented as mean ± standard deviation. One-way ANOVA was used for comparing multiple groups' data. ns, not significant, *$p < 0.05$, ***$p < 0.001$, ****$p < 0.0001$.

mained independently associated with 90-day mortality (HR: 0.696; 95% CI: 0.520–0.932; $p = 0.015$). Among the immunological variables included in the model, the proportion of M-MDSCs was the only immune cell subset that retained independent prognostic significance (Table 2).

3.6 Establishment of a CLP-Induced Murine Sepsis Model

To establish an experimental model corresponding to different phases of sepsis, a standard CLP procedure was performed in mice. Twelve hours post-CLP, mice showed significantly increased serum levels of the inflammatory cytokines IL-1β, IL-6, TNF and IL-10 compared to sham-operated controls (Fig. 4A–D).

Markers of cardiac injury, hepatic dysfunction, and renal impairment were also markedly increased at 12 hours post-CLP. By 7 days post-surgery, the levels of most inflammatory cytokines and organ injury markers had largely returned to the levels seen in the sham group (Fig. 4E–K).

3.7 Biphasic and Tissue-Specific Redistribution of MDSC Subsets in CLP-Induced Sepsis

MDSC percentages in the BM and spleens of mice were assessed at 12 h and 7 days post-CLP. Gating strategy MDSC subset (**Supplementary Fig. 2**). In the BM, MDSC dynamics exhibited a distinct pattern (Fig. 5D) such that at 12 hours after CLP modeling, the proportion of M-MDSCs significantly increased (Fig. 5B,F), whereas the proportion of P-MDSCs decreased compared to sham controls (Fig. 5B,E). By day 7, M-MDSC levels had partially declined but remained elevated compared with the sham group (Fig. 5A,C,F), whereas P-MDSC levels had markedly increased (Fig. 5C,E).

In the spleen, total MDSCs were significantly reduced at 12 hours post-CLP compared with sham controls (Fig. 6A,B,D), followed by a marked increase at 7 days (Fig. 6C). Subset analysis indicated that the early reduction was primarily attributable to a decrease in P-MDSCs (Fig. 6B,E), whereas the late increase was dominated by the expansion of M-MDSCs (Fig. 6C,F).

3.8 Sepsis Induces Tissue-Specific and Time-Dependent Activation of ER Stress-Related Signaling in MDSCs

To evaluate ER stress in MDSCs during sepsis, $CD11b^{+}Gr\text{-}1^{+}$ cells were extracted from the spleen and BM of both sham-operated mice and CLP model mice at 12 h and 7 days post-surgery. The purity of Gr-1 in mouse BM was verified using flow cytometry (**Supplementary Fig. 3**). Western blotting revealed elevated levels of ER stress-related proteins in MDSCs from CLP mice compared to sham controls. Specifically, in splenic $CD11b^{+}Gr\text{-}1^{+}$ cells, p-eIF2α/eIF2α was decreased, while Bip, XBP1, ATF4, and Nrf2 were significantly upregulated at 12 hours after CLP compared with the Sham group (Fig. 7A–E,G). whereas ATF6 levels showed an upward trend without statistical significance (Fig. 7A,F). At 7 days post-CLP, the expression of XBP1 (Fig. 7A,D), ATF4 (Fig. 7A,E), ATF6 (Fig. 7A,F), and Nrf2 (Fig. 7A,G) was significantly downregulated compared with the 12-hour time point. In contrast, p-eIF2α/eIF2α was decreased (Fig. 7C), Bip (Fig. 7B) and Nrf2 (Fig. 7G) levels remained significantly elevated relative to the Sham group, while ATF4 (Fig. 7E) levels remained numerically higher than the Sham group without reaching statistical significance.

In BM $CD11b^{+}Gr\text{-}1^{+}$ cells, Bip, XBP1, ATF4, and Nrf2 levels were significantly increased at 12 h after CLP compared with the Sham group (Fig. 8A–C,F,G). At 7 day, p-eIF2α/eIF2α was decreased (Fig. 8A,E), Bip (Fig. 8A,B), and Nrf2 (Fig. 8A,F) remained significantly elevated relative to the Sham group. Compared with the 12-h time point, the expression of Bip (Fig. 8A,B), XBP1 (Fig. 8A,C), ATF4 (Fig. 8A,G), and Nrf2 (Fig. 8A,F) was significantly decreased at 7 days, whereas ATF6 levels fluctuated among groups without statistical significance (Fig. 8A,D).

4. Discussion

In this prospective cohort study, we investigated the prognostic relevance of the percentage of circulating M-MDSCs in sepsis and explored their potential biological characteristics using a CLP-induced murine model. Circulating M-MDSCs significantly increased in sepsis patients within 24 hours of ICU admission. Higher proportions of M-MDSCs at admission were linked to better 90-day survival and independently correlated with mortality after adjusting for disease severity and other clinical variables. The same trend was observed in the bone marrow (12 hours post-CLP). Furthermore, the increase observed in patients was primarily driven by survivors, supporting the prognostic relevance of M-MDSCs. Third, in the CLP model, MDSC subsets exhibited distinct temporal and tissue-specific dynamics across the acute and recovery phases of sepsis. MDSCs isolated from septic mice showed activation of ER stress pathways in the spleen and bone marrow. Taken together, these findings suggest that early expansion of circulating M-MDSCs represents a prominent immunological feature of sepsis and may carry important prognostic information.

A key observation of this study is that among circulating MDSC subsets, only M-MDSCs differed significantly between survivors and non-survivors and retained independent prognostic value in multivariate analyses. While non-survivors exhibited higher severity scores and more pronounced systemic inflammation, the association between M-MDSC levels and clinical outcomes persisted after adjustment for these factors. This finding indicates that M-MDSCs may reflect aspects of host immune status that are not fully captured by conventional clinical severity indices. Our data is evident by highlighting the importance of focusing on the monocytic subset and on early time points in the disease course.

Sepsis is characterized by a complex and heterogeneous host response involving both excessive inflammation and immunosuppression [37,38,39]. A growing body of evidence indicates that MDSCs expand during sepsis and contribute to immune dysregulation [28,29,30]. Previous studies have linked persistent or delayed MDSC expansion to adverse outcomes, particularly in later phases of sepsis or septic shock [28,30], whereas other reports suggest that specific MDSC subsets may exert context-dependent regulatory effects [27]. In contrast, our study suggests that early expansion of M-MDSCs may be associated with improved clinical outcomes, highlighting the importance of temporal context when interpreting the role of MDSCs in sepsis [40].

From a biological perspective, M-MDSCs are known to exert diverse immunomodulatory effects, including regulation of T-cell activation, cytokine production, and myeloid cell differentiation [16,29]. This duality underscores the importance of temporal context in interpreting the immunological role of M-MDSCs. Rather than representing a uniform state of immune suppression, M-MDSC expansion during early sepsis may contribute to limiting excessive inflammatory injury and promoting immune homeostasis. Our experimental data from the CLP model support the concept that MDSC biology is highly dynamic, with marked redistribution and subset-specific expansion across immune compartments. The unique temporal patterns in the bone marrow and spleen highlight the complexity of myeloid cell responses during sepsis, indicating that circulating M-MDSC levels may reflect signals from various tissues.

Importantly, our clinical observations were paralleled by experimental findings in the CLP model. Increased M-MDSC levels were detected in the peripheral blood of patients during the early phase of sepsis and in the BM of septic mice at 12 h post-CLP. Moreover, in patients, this increase was predominantly observed in survivors, further supporting its potential prognostic relevance. At the tissue level, MDSC subsets displayed marked temporal and compartment-specific redistribution. In the spleen, early reductions in MDSC levels were mainly attributable to de-

creased P-MDSC abundance, whereas later expansion was dominated by M-MDSCs. In contrast, the BM exhibited early M-MDSC expansion followed by the recovery of P-MDSCs. These findings indicate that MDSC responses during sepsis are highly dynamic and tissue-dependent, and that circulating M-MDSCs may reflect broader myeloid reprogramming across immune compartments. This dynamic nature is also consistent with earlier experimental studies showing that MDSCs may either attenuate or aggravate inflammatory responses depending on the stage of sepsis and the subset involved [28,29].

An additional novel aspect of this study is the observation of ER stress activation in MDSCs during sepsis. In both spleen and BM derived $CD11b^{+}Gr\text{-}1^{+}$ cells, several canonical ER stress-related proteins, including Bip, p-eIF2α, XBP1, ATF4, and Nrf2, were upregulated during the acute phase following CLP. These findings indicate that MDSCs are exposed to substantial intracellular stress during sepsis, likely driven by the inflammatory milieu, hypoxia [41], and metabolic disturbances characteristic of this condition [42,43]. More broadly, ER stress and the unfolded protein response are increasingly recognized as important regulators of immune cell survival [44], differentiation [45], and signaling under inflammatory conditions [32,33,46,47].

Notably, ER stress activation in MDSCs exhibited pathway-selective and dynamic features. The PERK-eIF2α-ATF4 and IRE1-XBP1 branches of this pathway were prominently activated during the acute phase of sepsis, whereas ATF6 activation was relatively limited. In addition, ER stress marker levels were elevated at 12 h post-CLP and declined toward baseline at day 7, paralleling the attenuation of systemic inflammation. Differences between splenic and BM MDSCs further suggest that local microenvironmental factors may shape stress-response patterns in these cells. Taken together, these findings indicate that the sepsis-related induction of ER stress in MDSCs is not a uniform or sustained response, but rather a dynamic process characterized by pathway preference and tissue dependence.

Previous studies focused on cancer and inflammatory diseases have suggested that ER stress may influence the phenotype and functional properties of myeloid suppressor cells and other immunoregulatory myeloid populations [34,46,47]. In the present study, ER stress activation was observed in sepsis-associated MDSCs. However, whether this pathway directly regulates MDSC function in sepsis remains unclear. Therefore, the ER stress-related alterations identified here should be interpreted as associative rather than causal. Further mechanistic studies, including pharmacological inhibition or genetic modulation of ER stress pathways, are required to determine whether ER stress directly contributes to MDSC-mediated immune regulation in sepsis. The current study provides a solid foundation for subsequent mechanistic investigations.

Limitations should be acknowledged. First, reporting cell populations as percentages has inherent limitations, as the observed increase in MDSC proportions in sepsis may reflect underlying lymphopenia rather than a true increase in absolute MDSC numbers. Second, this study was conducted at a single center with a relatively modest sample size. Finally, although we identified ER stress activation in MDSCs in a murine model, direct functional assays linking ER stress pathways to M-MDSC immunoregulatory activity were not performed.

This study concludes that early expansion of circulating M-MDSCs independently correlates with enhanced 90-day survival in sepsis patients and highlights ER stress activation as a key biological characteristic of MDSCs in experimental sepsis. These findings underscore the intricate and context-specific role of M-MDSCs in sepsis, advocating for further research into their potential as immune biomarkers and therapeutic targets in critical illness.

5. Conclusions

The early increase of circulating M-MDSCs is independently linked to enhanced 90-day survival in sepsis patients. The study underscores the variable role of M-MDSCs in sepsis, indicating that early immunoregulatory responses, possibly associated with ER stress activation, could lead to positive clinical outcomes.

Availability of Data and Materials

The datasets used and analyzed during the current study are available from the corresponding author on reasonable request.

Author Contributions

JLL contributed to study design, evaluated abdominal inflammation and survival outcomes in CLP models, and characterized immune cell surface markers using flow cytometry, acquired funding, and participated in both the original draft writing and the review and editing process. TNWR contributed to resources by preparing bone marrow MDSCs and splenocyte single suspension, and was responsible for magnetic cell separation and subsequent FACS staining. XYS assisted CLP surgery, and conducted protein expression analysis via western blotting. XS prepared tissue samples and collected the basic information of the patients. SQM project administration, Conceptualization. RLG supervised and controlled the overall experimental quality, designed the experimental workflow, and oversaw the research process—including data acquisition, analysis, and interpretation. All authors contributed to editorial changesin the manuscript. All authors read and approved the final manuscript. All authors have participated sufficientlyin the work and agreed to be accountable for all aspects ofthe work.

Ethics Approval and Consent to Participate

The protocol of this study was approved by the Ethics Committee of Qinghai Provincial People's Hospital [Approval No. (2023)-247] and in accordance with the Declaration of Helsinki. All participants were fully informed about the study's purpose and procedures, and each provided written informed consent. All animal experiments were approved by the Institutional Animal Care and Use Committee of Qinghai Provincial People's Hospital (Approval No. [2024]-020) and were conducted in accordance with the ARRIVE guidelines 2.0 for reporting animal research.

Acknowledgment

We sincerely thank Huifang Liu and Qiying Xu for their valuable guidance in flow cytometry modeling and related procedures. We are also deeply grateful to all the patients who participated in this study.

Funding

This work was supported by grants from 2020 Qinghai Provincial Health Commission Guiding Topic (2020-wjzdx-01) and Qinghai Province "Kunlun Talents High-end Innovative and Entrepreneurial Talents" cultivate top-notch talent (QHKLYC-GDCXCY-2024-130).

Conflicts of Interest

The authors declare no conflicts of interest.

Supplementary Material

Supplementary material associated with this article can be found, in the online version, at https://doi.org/10.31083/FBL50593.

References

[1] Singer M, Deutschman CS, Seymour CW, Shankar-Hari M, Annane D, Bauer M, et al. The Third International Consensus Definitions for Sepsis and Septic Shock (Sepsis-3). JAMA. 2016; 315: 801–810. https://doi.org/10.1001/jama.2016.0287

[2] Singer M, Angus DC, Annane D, Bauer M, Kalil AC, Klompas M, et al. Sepsis. Lancet. 2026; 407: 1276–1288. https://doi.org/10.1016/S0140-6736(25)02422-5

[3] Rudd KE, Johnson SC, Agesa KM, Shackelford KA, Tsoi D, Kievlan DR, et al. Global, regional, and national sepsis incidence and mortality, 1990-2017: analysis for the Global Burden of Disease Study. Lancet. 2020; 395: 200–211. https://doi.org/10.1016/S0140-6736(19)32989-7

[4] Fleischmann-Struzek C, Mellhammar L, Rose N, Cassini A, Rudd KE, Schlattmann P, et al. Incidence and mortality of hospital- and ICU-treated sepsis: results from an updated and expanded systematic review and meta-analysis. Intensive Care Medicine. 2020; 46: 1552–1562. https://doi.org/10.1007/s00134-020-06151-x

[5] Willmann K, Moita LF. Physiologic disruption and metabolic reprogramming in infection and sepsis. Cell Metabolism. 2024; 36: 927–946. https://doi.org/10.1016/j.cmet.2024.02.013

[6] van der Poll T, van de Veerdonk FL, Scicluna BP, Netea MG. The immunopathology of sepsis and potential therapeutic targets. Nature Reviews. Immunology. 2017; 17: 407–420. https://doi.org/10.1038/nri.2017.36

[7] Hotchkiss RS, Swanson PE, Freeman BD, Tinsley KW, Cobb JP, Matuschak GM, et al. Apoptotic cell death in patients with sepsis, shock, and multiple organ dysfunction. Critical Care Medicine. 1999; 27: 1230–1251. https://doi.org/10.1097/00003246-199907000-00002

[8] Monneret G, Lepape A, Voirin N, Bohé J, Venet F, Debard AL, et al. Persisting low monocyte human leukocyte antigen-DR expression predicts mortality in septic shock. Intensive Care Medicine. 2006; 32: 1175–1183. https://doi.org/10.1007/s00134-006-0204-8

[9] Meisel C, Schefold JC, Pschowski R, Baumann T, Hetzger K, Gregor J, et al. Granulocyte-macrophage colony-stimulating factor to reverse sepsis-associated immunosuppression: a double-blind, randomized, placebo-controlled multicenter trial. American Journal of Respiratory and Critical Care Medicine. 2009; 180: 640–648. https://doi.org/10.1164/rccm.200903-0363OC

[10] Lin Y, Liu L, Liu Y, Yang R, Liao S, Xu M, et al. MiR-145 Alleviates Sepsis-Induced Inflammatory Responses and Organ Injury by Targeting ADAM17. Frontiers in Bioscience (Landmark Edition). 2024; 29: 44. https://doi.org/10.31083/j.fbl2901044

[11] Boomer JS, To K, Chang KC, Takasu O, Osborne DF, Walton AH, et al. Immunosuppression in patients who die of sepsis and multiple organ failure. JAMA. 2011; 306: 2594–2605. https://doi.org/10.1001/jama.2011.1829

[12] Hotchkiss RS, Monneret G, Payen D. Immunosuppression in sepsis: a novel understanding of the disorder and a new therapeutic approach. The Lancet. Infectious Diseases. 2013; 13: 260–268. https://doi.org/10.1016/S1473-3099(13)70001-X

[13] Gabrilovich DI, Nagaraj S. Myeloid-derived suppressor cells as regulators of the immune system. Nature Reviews. Immunology. 2009; 9: 162–174. https://doi.org/10.1038/nri2506

[14] Veglia F, Sanseviero E, Gabrilovich DI. Myeloid-derived suppressor cells in the era of increasing myeloid cell diversity. Nature Reviews. Immunology. 2021; 21: 485–498. https://doi.org/10.1038/s41577-020-00490-y

[15] Bronte V, Brandau S, Chen SH, Colombo MP, Frey AB, Greten TF, et al. Recommendations for myeloid-derived suppressor cell nomenclature and characterization standards. Nature Communications. 2016; 7: 12150. https://doi.org/10.1038/ncomms12150

[16] Rodriguez PC, Ernstoff MS, Hernandez C, Atkins M, Zabaleta J, Sierra R, et al. Arginase I-producing myeloid-derived suppressor cells in renal cell carcinoma are a subpopulation of activated granulocytes. Cancer Research. 2009; 69: 1553–1560. https://doi.org/10.1158/0008-5472.CAN-08-1921

[17] Bronte V, Serafini P, Mazzoni A, Segal DM, Zanovello P. L-arginine metabolism in myeloid cells controls T-lymphocyte functions. Trends in Immunology. 2003; 24: 302–306. https://doi.org/10.1016/s1471-4906(03)00132-7

[18] Rastad JL, Green WR. Myeloid-derived suppressor cells in murine AIDS inhibit B-cell responses in part via soluble mediators including reactive oxygen and nitrogen species, and TGF-β. Virology. 2016; 499: 9–22. https://doi.org/10.1016/j.virol.2016.08.031

[19] He YM, Li X, Perego M, Nefedova Y, Kossenkov AV, Jensen EA, et al. Transitory presence of myeloid-derived suppressor cells in neonates is critical for control of inflammation. Nature Medicine. 2018; 24: 224–231. https://doi.org/10.1038/nm.4467

[20] Tebartz C, Horst SA, Sparwasser T, Huehn J, Beineke A, Peters G, et al. A major role for myeloid-derived suppressor cells and a minor role for regulatory T cells in immunosuppression during Staphylococcus aureus infection. Journal of Immunology. 2015; 194: 1100–1111. https://doi.org/10.4049/jimmunol.1400196

[21] Heim CE, Vidlak D, Scherr TD, Kozel JA, Holzapfel M, Muir-

head DE, et al. Myeloid-derived suppressor cells contribute to Staphylococcus aureus orthopedic biofilm infection. Journal of Immunology. 2014; 192: 3778–3792. https://doi.org/10.4049/jimmunol.1303408

[22] Zhang C, Lei GS, Shao S, Jung HW, Durant PJ, Lee CH. Accumulation of myeloid-derived suppressor cells in the lungs during Pneumocystis pneumonia. Infection and Immunity. 2012; 80: 3634–3641. https://doi.org/10.1128/IAI.00668-12

[23] Sander LE, Sackett SD, Dierssen U, Beraza N, Linke RP, Müller M, et al. Hepatic acute-phase proteins control innate immune responses during infection by promoting myeloid-derived suppressor cell function. The Journal of Experimental Medicine. 2010; 207: 1453–1464. https://doi.org/10.1084/jem.20091474

[24] Mathias B, Delmas AL, Ozrazgat-Baslanti T, Vanzant EL, Szpila BE, Mohr AM, et al. Human Myeloid-derived Suppressor Cells are Associated With Chronic Immune Suppression After Severe Sepsis/Septic Shock. Annals of Surgery. 2017; 265: 827–834. https://doi.org/10.1097/SLA.0000000000001783

[25] Waeckel L, Venet F, Gossez M, Monard C, Rimmelé T, Monneret G. Delayed persistence of elevated monocytic MDSC associates with deleterious outcomes in septic shock: a retrospective cohort study. Critical Care. 2020; 24: 132. https://doi.org/10.1186/s13054-020-02857-y

[26] Hollen MK, Stortz JA, Darden D, Dirain ML, Nacionales DC, Hawkins RB, et al. Myeloid-derived suppressor cell function and epigenetic expression evolves over time after surgical sepsis. Critical Care. 2019; 23: 355. https://doi.org/10.1186/s13054-019-2628-x

[27] Schrijver IT, Karakike E, Théroude C, Baumgartner P, Harari A, Giamarellos-Bourboulis EJ, et al. High levels of monocytic myeloid-derived suppressor cells are associated with favorable outcome in patients with pneumonia and sepsis with multi-organ failure. Intensive Care Medicine Experimental. 2022; 10: 5. https://doi.org/10.1186/s40635-022-00431-0

[28] Brudecki L, Ferguson DA, McCall CE, El Gazzar M. Myeloid-derived suppressor cells evolve during sepsis and can enhance or attenuate the systemic inflammatory response. Infection and Immunity. 2012; 80: 2026–2034. https://doi.org/10.1128/IAI.00239-12

[29] Cuenca AG, Delano MJ, Kelly-Scumpia KM, Moreno C, Scumpia PO, Laface DM, et al. A paradoxical role for myeloid-derived suppressor cells in sepsis and trauma. Molecular Medicine. 2011; 17: 281–292. https://doi.org/10.2119/molmed.2010.00178

[30] Janols H, Bergenfelz C, Allaoui R, Larsson AM, Rydén L, Björnsson S, et al. A high frequency of MDSCs in sepsis patients, with the granulocytic subtype dominating in gram-positive cases. Journal of Leukocyte Biology. 2014; 96: 685–693. https://doi.org/10.1189/jlb.5HI0214-074R

[31] van der Poll T. Myeloid-derived Suppressor Cells in Sepsis. American Journal of Respiratory and Critical Care Medicine. 2017; 196: 256–258. https://doi.org/10.1164/rccm.201701-0046ED

[32] Grootjans J, Kaser A, Kaufman RJ, Blumberg RS. The unfolded protein response in immunity and inflammation. Nature Reviews. Immunology. 2016; 16: 469–484. https://doi.org/10.1038/nri.2016.62

[33] Walter P, Ron D. The unfolded protein response: from stress pathway to homeostatic regulation. Science. 2011; 334: 1081–1086. https://doi.org/10.1126/science.1209038

[34] Cubillos-Ruiz JR, Silberman PC, Rutkowski MR, Chopra S, Perales-Puchalt A, Song M, et al. ER Stress Sensor XBP1 Controls Anti-tumor Immunity by Disrupting Dendritic Cell Homeostasis. Cell. 2015; 161: 1527–1538. https://doi.org/10.1016/j.cell.2015.05.025

[35] Rittirsch D, Huber-Lang MS, Flierl MA, Ward PA. Immunodesign of experimental sepsis by cecal ligation and puncture. Nature Protocols. 2009; 4: 31–36. https://doi.org/10.1038/nprot.2008.214

[36] Autengruber A, Gereke M, Hansen G, Hennig C, Bruder D. Impact of enzymatic tissue disintegration on the level of surface molecule expression and immune cell function. European Journal of Microbiology & Immunology. 2012; 2: 112–120. https://doi.org/10.1556/EuJMI.2.2012.2.3

[37] Bone RC. Sir Isaac Newton, sepsis, SIRS, and CARS. Critical Care Medicine. 1996; 24: 1125–1128. https://doi.org/10.1097/00003246-199607000-00010

[38] Osuchowski MF, Welch K, Siddiqui J, Remick DG. Circulating cytokine/inhibitor profiles reshape the understanding of the SIRS/CARS continuum in sepsis and predict mortality. Journal of Immunology. 2006; 177: 1967–1974. https://doi.org/10.4049/jimmunol.177.3.1967

[39] Zhu B, Wang J, Wang Y. Multi-omics Analysis Reveals Molecular Subtype of Mitochondrial Oxidative Stress and Prognostic Model Development in Sepsis. Frontiers in Bioscience (Landmark Edition). 2025; 30: 38957. https://doi.org/10.31083/fbl38957

[40] Veglia F, Perego M, Gabrilovich D. Myeloid-derived suppressor cells coming of age. Nature Immunology. 2018; 19: 108–119. https://doi.org/10.1038/s41590-017-0022-x

[41] Luo Z, Tian M, Yang G, Tan Q, Chen Y, Li G, et al. Hypoxia signaling in human health and diseases: implications and prospects for therapeutics. Signal Transduction and Targeted Therapy. 2022; 7: 218. https://doi.org/10.1038/s41392-022-01080-1

[42] Di Conza G, Ho PC, Cubillos-Ruiz JR, Huang SCC. Control of immune cell function by the unfolded protein response. Nature Reviews. Immunology. 2023; 23: 546–562. https://doi.org/10.1038/s41577-023-00838-0

[43] Cláudio N, Dalet A, Gatti E, Pierre P. Mapping the crossroads of immune activation and cellular stress response pathways. The EMBO Journal. 2013; 32: 1214–1224. https://doi.org/10.1038/emboj.2013.80

[44] Hetz C, Zhang K, Kaufman RJ. Mechanisms, regulation and functions of the unfolded protein response. Nature Reviews. Molecular Cell Biology. 2020; 21: 421–438. https://doi.org/10.1038/s41580-020-0250-z

[45] Condamine T, Kumar V, Ramachandran IR, Youn JI, Celis E, Finnberg N, et al. ER stress regulates myeloid-derived suppressor cell fate through TRAIL-R-mediated apoptosis. The Journal of Clinical Investigation. 2014; 124: 2626–2639. https://doi.org/10.1172/JCI74056

[46] Hetz C, Papa FR. The Unfolded Protein Response and Cell Fate Control. Molecular Cell. 2018; 69: 169–181. https://doi.org/10.1016/j.molcel.2017.06.017

[47] Cubillos-Ruiz JR, Bettigole SE, Glimcher LH. Tumorigenic and Immunosuppressive Effects of Endoplasmic Reticulum Stress in Cancer. Cell. 2017; 168: 692–706. https://doi.org/10.1016/j.cell.2016.12.004